Vol. 23(2) : 161~172 | Ocean and Polar Research | June 2001

POM/MICOM Inter-Comparison in Modeling the East Sea Circulation

Kuk-Jin Kim*[1], Young-Ho Seung[1], and Moon-Sik Suk[2]

[1]*Department of Oceanography, Inha University*
Incheon 402-751, Korea
[2]*Marine Environment and Climate Change Laboratory, KORDI*
Ansan P.O. Box 29, Seoul 425-600, Korea

Abstract : A model-to-model comparison is attempted between Princeton Ocean Model (POM) and Miami Isopycnic Coordinate Ocean Model (MICOM) as a first step to extend our knowledge of models' performances in studying the East Sea circulation. The two models have fundamentally different numerical schemes and boundary conditions imposed on these models are not exactly the same each other. This study indicates that MICOM has a critical weak point in that it does not reproduce the shallow surface currents properly while it handles the thermohaline processes and associated movements of intermediate and deep waters efficiently. It is suggested that the mixed layer scheme needs to be modified so that it can match with inflow boundary conditions in order to reproduce the surface currents properly in MICOM. POM reproduces the surface current pattern better than MICOM, although the surface currents in POM appear to undergo the unrealistic seasonal variation and have exaggeratedly large vertical scale. These defects seem to arise during the process of adapting POM to the East Sea, and removing these defects is left as a future task.

Key words : POM / MICOM, model comparison, East Sea circulation.

1. Introduction

The East Sea has been known to be a good place to study oceanic processes economically because it has a relatively small dimension while being rich in oceanic processes. For this reason and another, there are more and more oceanographers attracted to this small basin. The general features of the East Sea circulation deduced from many observations can be summarized as follows (e.g. Moriyasu 1972). A warm surface water is carried into the East Sea by the Tsushima Current (hereafter, TC) through the Korea Strait. A part of it called the Nearshore Branch (hereafter, NB) flows along the Japanese coast, the second branch flows to the same direction as the NB just offshore of the NB (Kawabe 1982), and the East Korean Warm Current (hereafter, EKWC) flows northward along the Korean coast. Yoon (1982a, 1982b) suggested that the NB is topographically controlled and the EKWC is generated due to the planetary β effect. The EKWC separates from the coast near 38°N, and moves eastward toward the Tsugaru and Soya Straits where it flows out to the North Pacific. North of the warm current region, a cold current called the North Korean Cold Current (hereafter, NKCC) or the Liman Current (hereafter, LC) flows southward along the Korean coast and meets with the EKWC to form a polar front (Fig. 1). Seung (1992) shows analytically that the cold current is driven by wind and surface cooling. It has been believed that the NB and EKWC strengthen in summer due to the increase in either the baroclinicity or the volume transport through the Korea Strait (e.g. Lee *et al.* 1997), and the NKCC / LC strengthens in winter due to the strong northwesterly wind. However, this is only a rough description of the actual

* Corresponding author. E-mail : g93420950@inhavision.inha.ac.kr

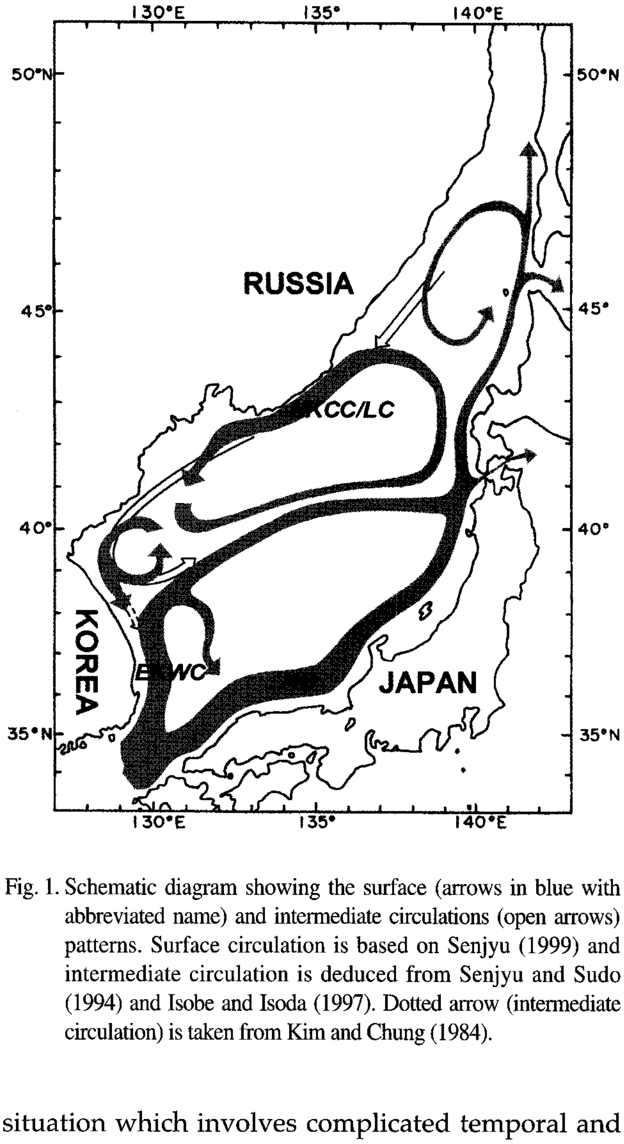

Fig. 1. Schematic diagram showing the surface (arrows in blue with abbreviated name) and intermediate circulations (open arrows) patterns. Surface circulation is based on Senjyu (1999) and intermediate circulation is deduced from Senjyu and Sudo (1994) and Isobe and Isoda (1997). Dotted arrow (intermediate circulation) is taken from Kim and Chung (1984).

situation which involves complicated temporal and spatial variations with vigorous eddy activities.

The East Sea Intermediate Water (hereafter, ESIW) characterized by low salinity and high oxygen contents occupies a relatively thin layer below the warm surface waters carried by the EKWC and NB (Kim and Chung 1984; Kim *et al.* 1991). The ESIW is thought to be formed at the surface in the northwestern part of the basin and flows southward along the Korean coast as a part of the cyclonic recirculation gyre north of the polar front (Senjyu and Sudo 1993, 1994; Seung and Yoon 1995a; Isobe and Isoda 1997; Fig. 1). The southward extension of the ESIW is evidenced by its presence off Korean coast and the cyclonic recirculation of it results in a doming structure with fresh water around the dome (Isobe and Isoda 1997; Fig. 13 in Kim and Seung 1999). These results provide an idea, though rough, of the intermediate circulation in the East Sea which has not long been figured out.

Below the ESIW layer, a very deep, cold and nearly homogeneous water called the East Sea Proper Water (hereafter, ESPW) occupies the rest of the water column. Recent CREAMS observations (Kim *et al.* 1996; Kim and Kim 1996) reveal that the ESPW is not a single water mass and there exists a deep salinity minimum layer with high oxygen contents around the depth 1000-2000 m, although the low salinity character of this water is much weaker than that of the ESIW. They named it as the East Sea Deep Intermediate Water in distinction from the ESIW. Circulation of the deep water is poorly known. The deep current (600-800 m depth) off Korean coast is toward the southeast in summer season with magnitude of a few cm / sec (Lie *et al.* 1989). Results of moored current measurements conducted in the Japan Basin located in the northern part of the East Sea, and in the Ulleung Basin located in the southwestern part of the East Sea, indicate that bottom currents are much stronger than expected, reaching to 10 cm / s at times (Takematsu *et al.* 1999; K.-I. Chang, personal communication). They exhibit eddy-like fluctuations and bottom-intensification occurred at some locations. Holloway *et al.* (1995) suggest that strong bottom flow is induced by the interaction between bottom pressure and topography, the topostress in their terminology. Whereas Hogan and Hurlbert (2000) attribute the strong bottom currents to the baroclinic instability and topography.

Many numerical experiments have been performed in the East Sea since Yoon (1982a, b and c). Later, Seung and Kim (1993), Seung and Yoon (1995b), Kim and Yoon (1999), Ro (1999), and Chu *et al.* (1999) have successfully reproduced the major features of the surface circulation of the East Sea. However, modeling the intermediate / deep circulations have not always been successful. Recently, Kim and Seung (1999) and Yoshikawa *et al.* (1999) focused on the intermediate water and reproduced the formation and circulation of the ESIW satisfactorily. According to their model results, the ESIW is formed in the northwestern part of the East Sea and circulates cyclonically around the northern / northwestern half of the basin. Numerical models used in the above studies include the Bryan-Cox type (Bryan and Cox 1969; Cox 1984), the Princeton Ocean Model (hereafter POM, Mellor and Blumberg 1985), and the Miami Isopycnic Coordinate Ocean

Model (hereafter, MICOM) used by Kim and Seung (1999). The major difference of those models lies in the vertical coordinates used. The Bryan-Cox type and the princeton Ocean Model use the Cartesian coordinate (z-coordinate) and the σ-coordinate, respectively, while the MICOM employs the isopycnic coordinate. MICOM takes the advantage of the fact that most of the oceanic processes occur along isopycnic surfaces. The uppermost layer overlying the isopycnic layers is treated as a single mixed layer that evolves according to the classical mixed layer theory (Krauss and Turner 1967). Hence, the MICOM mainly aims to reproduce the processes taking place in the ocean interior rather than in the shallow surface layer or coastal regions. POM is widely used in both coastal and oceanic circulation problems, and a turbulence closure scheme is used in transferring the thermal and mechanical effects imposed at the surface boundary to deeper layers. However, POM is known to have some troubles, like other σ-coordinate models, in the presence of steep bathymetry, especially if the grid spacing is not fine enough. Any of these models can be used in modeling the East Sea circulation. However, each model has its own character and it is not yet known how these different characters have effects on modeling the East Sea circulation. An inter-comparison between different types of models is necessary, and as a first step toward this goal, the comparison between POM and MICOM is attempted here.

2. Models

Model configuration, boundary conditions, viscosity coefficients, climatological surface flux data used in each model are listed in Table 1. Results from POM are those obtained by applying it to the Northwestern Pacific, whereas results from MICOM are obtained by applying it directly to the East Sea with the conditions as close as those employed in POM. It is quite difficult to impose exactly the same conditions as those in POM on the open boundaries of MICOM because the two models are different both in the vertical resolution and the treatment of the uppermost layer. Using the temperature and salinity from POM, the inflow open boundary condition is specified in the same manner as was used by Kim and Seung(1999; hereafter KS) with MICOM, that is, the TC water is assumed to have fixed temperature and salinity between 50-100 m depth at the inflow boundary. Temperature and salinity in the mixed layer between 0-50 m depth at the inflow boundary are then determined in such a way that the total heat and salt contained in the water column are conserved. Later, salinity within each isopycnic layer, including the TC water, is allowed to vary in response to thermohaline forcing imposed at the surface while retaining the same density. Temperature, salinity, and density in the mixed layer as well as the mixed layer depth change according to the mixed layer algorithm proposed by Krauss and

Table 1. Various conditions applied to POM and MICOM.

	POM	MICOM
Horizontal Resolution	0.2° ×0.2°	0.2° ×0.2°
Vertical Resolution	18 σ-levels	10 layers
Inflow Open Boundary Condition	2.3 Sv	transport : barotropic current 2.3 Sv uniform horizontally
Outflow Open Boundary Condition	Tsugaru St. : 90% of inflow transport Soya St. : 10% of inflow transport radiation condition	Tsugaru St. : 90% of inflow transport Soya St. : 10% of inflow transport radiation condition
Horizontal Eddy Viscosity	3×10^5 cm^2s^{-1} + Smagorinsky with coefficient 0.13	max of [5×10^5 cm^2s^{-1}, Smagorinsky with coefficient 0.1]
Vertical Eddy Viscosity	turbulence closure scheme	diapycnal mixing with constant vertical eddy viscosity
Wind	Hellerman-Rosenstein wind (1983)	Hellerman-Rosenstein wind (1983)
Surface T & S	relaxation of JODC dataset	relaxation of JODC dataset

Turner (1967). The volume transport obtained in POM changes little with time so that constant volume transport is imposed at open boundaries of MICOM. Other conditions for MICOM are the same as those in KS. Although these models do not have exactly the same conditions, they are expected to generate the nearly same general features which our study focuses on. It is also expected that motions induced below the surface layer by local forcing such as wind and surface cooling would not be greatly affected by the difference in the open boundary conditions mentioned above. Horizontal eddy viscosity is larger in POM than in MICOM, although it is on the order of 10^6 cm^2/s for both models. Bottom topography is based on the etopo-5 data for both models.

3. Model results

Comparisons are made for surface, intermediate and deep circulations with salinity distribution at the intermediate depth, and for the velocity and salinity distributions on two vertical sections: one approximately along 38°N (106 line in Fig. 2), and the other crossing the center of the basin (PM line in Fig. 2). Winter and summer seasons in the following text represent January and July, respectively. Surface and intermediate circulations calculated from both models are compared with the schematic circulation pattern shown in Fig. 1. Model-generated deep currents are compared with those observed. On two vertical sections, examinations are focused on the distribution of ESIW and its circulation in comparison with the aforementioned observations.

Surface circulation

The most prominent feature of the surface circulation in the East Sea is the presence of the NB, EKWC and NKCC/LC, and that the NB and the EKWC are strongest in summer and the NKCC/LC is strongest in winter. Despite the difference in the inflow boundary condition between the two models, they both show the presence of NB, EKWC and NKCC/LC (Fig. 2) similar to those depicted in Fig. 1. However, detailed examinations show some differences between the two models. Contrary to what is believed, the NKCC/LC and the NB from MICOM are stronger in summer and in winter, respectively. It seems to result from the wind climatology used here, since the NKCC/LC becomes stronger in winter in KS who used different wind climatology. The surface circulation in POM seems to be better reproduced as compared to that in MICOM. However, it is somewhat different from other model results obtained from the z-coordinate models such as those by Seung and Kim (1993) and Kim and Yoon (1999). Although direct comparisons between these model results and those obtained by POM are not possible due to different conditions applied, the results from POM are characterized by the broader EKWC, weaker EKWC in summer, and the relatively stronger NKCC/LC in summer as compared to those from the other z-coordinate models. The development of relatively stronger NKCC/LC in summer is also observed in MICOM, and seems to be due to the wind climatology employed here. The broader EKWC in POM may partly arises from the large horizontal eddy viscosity used. However, it is not understood why the EKWC is not strong in summer. It may be probably due to the fact that POM was configured to the entire Northwestern Pacific rather than only to the East Sea.

It should be noted that there exists a fundamental difference in numerical scheme between the two models. The isopycnic coordinate models like MICOM have layer thicknesses varying with time, and accurate open boundary conditions should involve both the layer thickness and physical parameters in each layer. Therefore, it is almost impossible to use the POM results as the boundary conditions of MICOM. The density of the inflowing TC water changes slightly with time in POM, while the density remains unchanged in MICOM because it is treated as an isopycnic layer. To correctly reflect the density change of the inflowing TC, the TC should be incorporated into the mixed layer with many thin sub-layers that is technically difficult in MICOM. Overall, the isopycnic coordinate models like MICOM are not suitable in modeling shallow surface currents like TC, and it is especially so when the model interior is highly dependent on open boundary conditions.

Intermediate/deep circulation

MICOM successfully reproduces the cyclonic recirculation of the intermediate layer in the northwestern part of the basin (Fig. 3). The distribution of salinity indicates that the low salinity water is carried by this circulation. The current becomes slightly stronger in summer. Compared with the KS's results, it shows less southward extension, probably because of the different

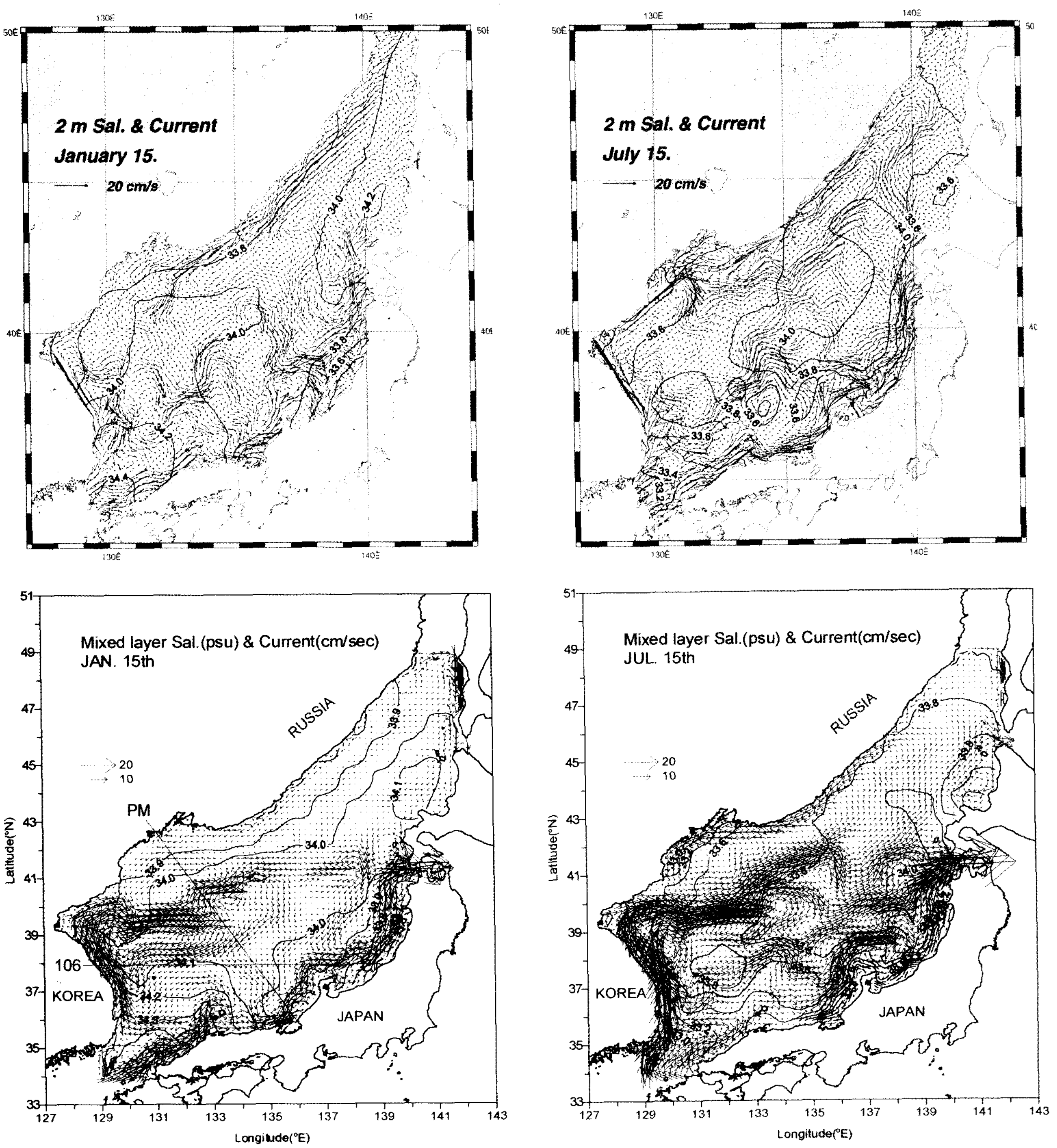

Fig. 2. Surface currents obtained by POM (upper) and MICOM (lower) in January and July. Two straight lines denote PM and 106 lines. Salinity contours are overlaid.

wind climatology employed here. POM fails to produce this tendency. Instead, it shows northward flow all along the Korean coast both in winter and summer.

Deep currents obtained in POM and MICOM have the magnitude on the order of 1 cm / s with the former slightly stronger than the latter (Fig. 4). The strong currents like those observed by Takematsu *et al.* (1999) are not seen probably because these models cannot generate either baroclinic instability or topostress which gives rise to strong bottom current as suggested, respectively,

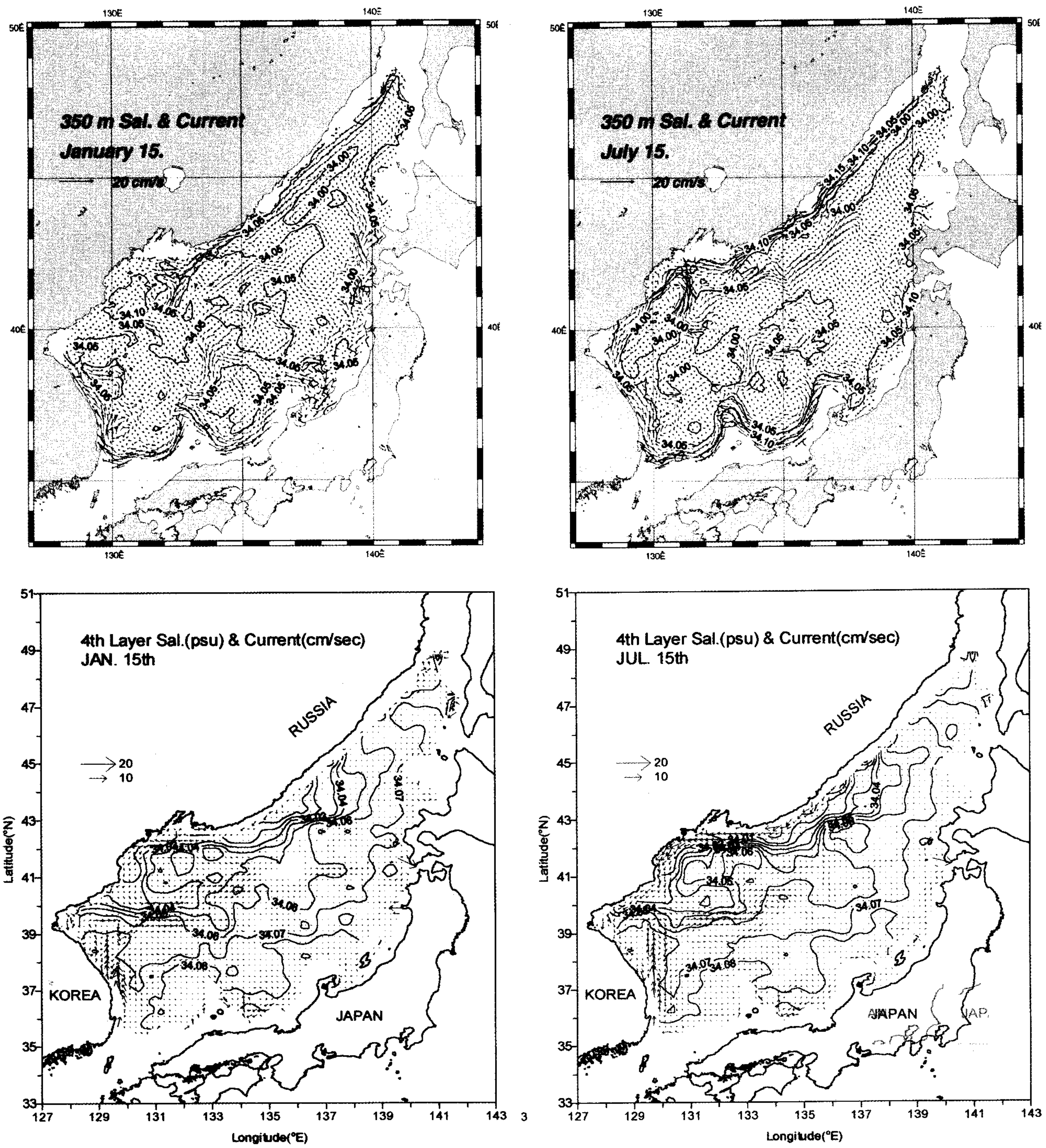

Fig. 3. Distributions of current (arrows) and salinity (contours) in intermediate layer obtained by POM (upper) and MICOM (lower) in January and July. Depth for MICOM is approximately the same as that for POM.

by Hogan and Hurlbert (2000) and Holloway *et al.* (1995). According to them, finer horizontal grid resolution or special parameterization is needed to obtain strong deep currents.

Vertical sections

A great difference between the two models can be seen on the salinity section along the PM line (Fig. 5). It is clear in MICOM that the low salinity water, repre-

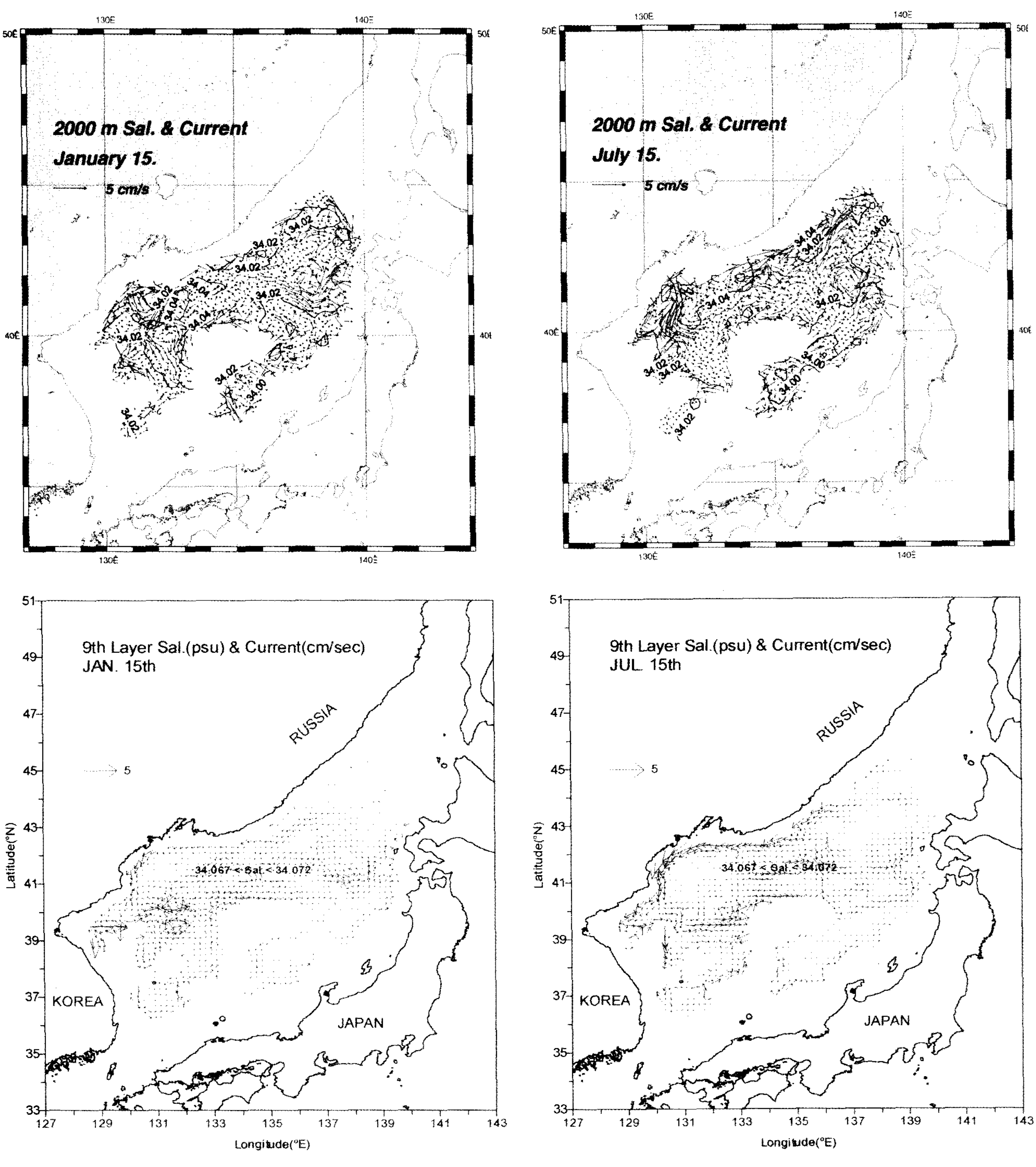

Fig. 4. Same as Fig. 3 except for deep current. Salinity is nearly homogeneous for MICOM and is not plotted.

senting the ESIW, usually presents north of 42° N extending from the surface to depth of about 500 m. It extends southward to about 39° N in winter. In summer, it is also found in the south but is not connected to the low salinity water in the north. The north-south distribution of this water mass is such that it creates a doming of lower deep water at the mid-point of it. The velocity distribution along the same section (Fig. 6) shows that the low salinity water is carried cyclonically around the dome by the NKCC/LC. In the north, the low salin-

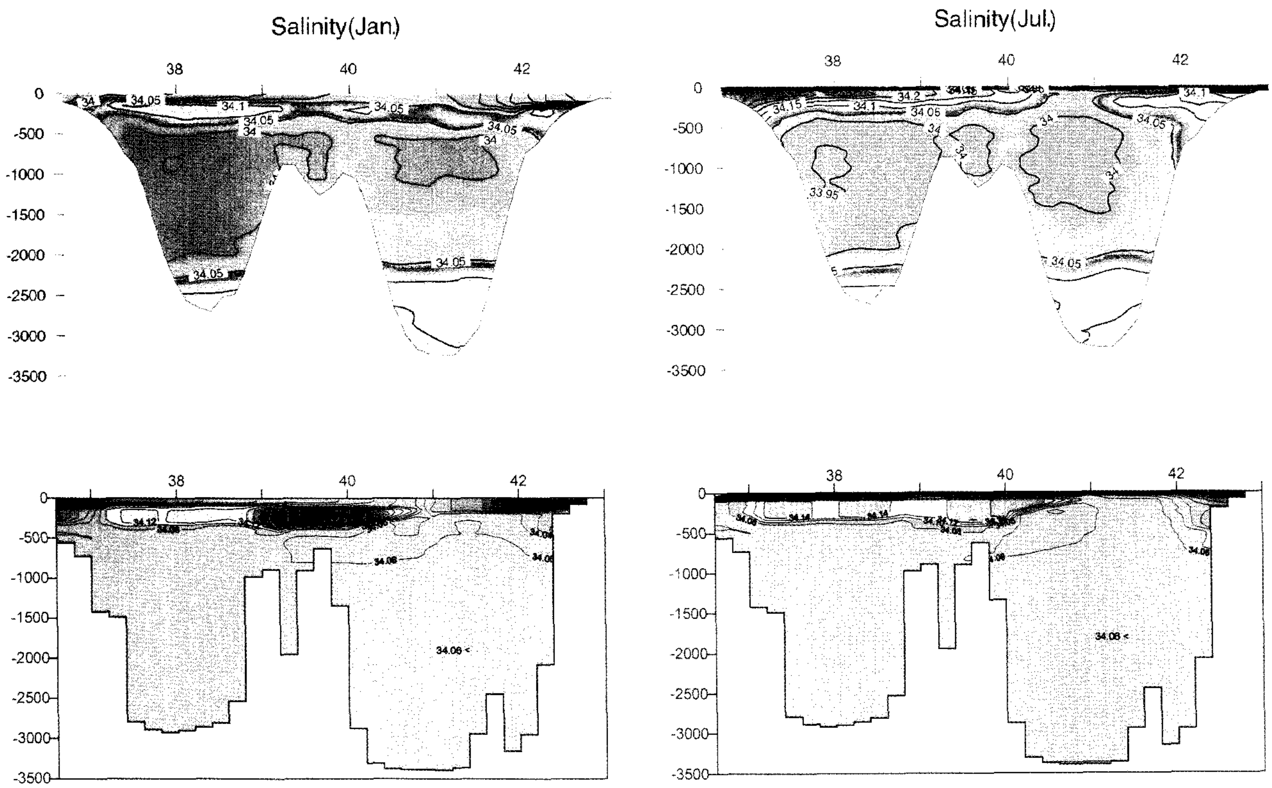

Fig. 5. Distribution of salinity (psu) on the vertical section along PM line for POM (upper) and MICOM (lower) in January and July. Ordinate is in meter and abscissa is in° N. Salinity increases from blue to red via yellow.

ity water is carried by a deep surface current but in the south, the major part of it is carried by a subsurface current just below the warm surface current which flows in the same direction. In POM, the low salinity water occupies major of the water column between surface and bottom waters with higher salinity than that in MICOM (Fig. 5). The low salinity water in POM is not considered to be the ESIW. Furthermore, the POM results do not show any organized flow pattern (Fig. 6) like the cyclonic circulation observed in MICOM. In MICOM, the ESIW and associated circulation of it are the results of the specification of low salinity as the surface boundary condition along the northern Russian coast, as shown in KS. Hence, the absence of these features in POM suggests the inefficiency of POM to respond to the thermohaline forcing.

The eastward (out of the page in Fig. 6) surface current with underlying countercurrent south of 37.0-37.5° N near Japanese coast, and the westward (into the page) current with a large vertical extent around 42° N near Russian coast are common features for both models. Note that the underlying countercurrent near Japanese coast has been observed (Hase *et al.* 1999) and confirmed in some numerical models (e.g. Seung and Kim 1993; Kim and Yoon 1999). The surface current near Russian coast appears to have the large vertical extent because of the weak vertical stratification.

In general, POM generates stronger currents than MICOM (Fig. 6). Especially, the undercurrent found near Japanese coast seems to be bottom-intensified, showing a strong baroclinic structure over the sloping bottom. The vertical structure of the NKCC/LC obtained in MICOM seems to be somewhat counterintuitive in that it has a deep penetrating structure and strong in summer rather than in winter. This seems to be related with the abnormally stronger NKCC/LC in summer observed in the surface current distribution in MICOM.

On the salinity section along the 106 line, POM shows the presence of low salinity water with large vertical and horizontal extents (Fig. 7) as observed on PM line. In MICOM, it appears only in the confined area near the

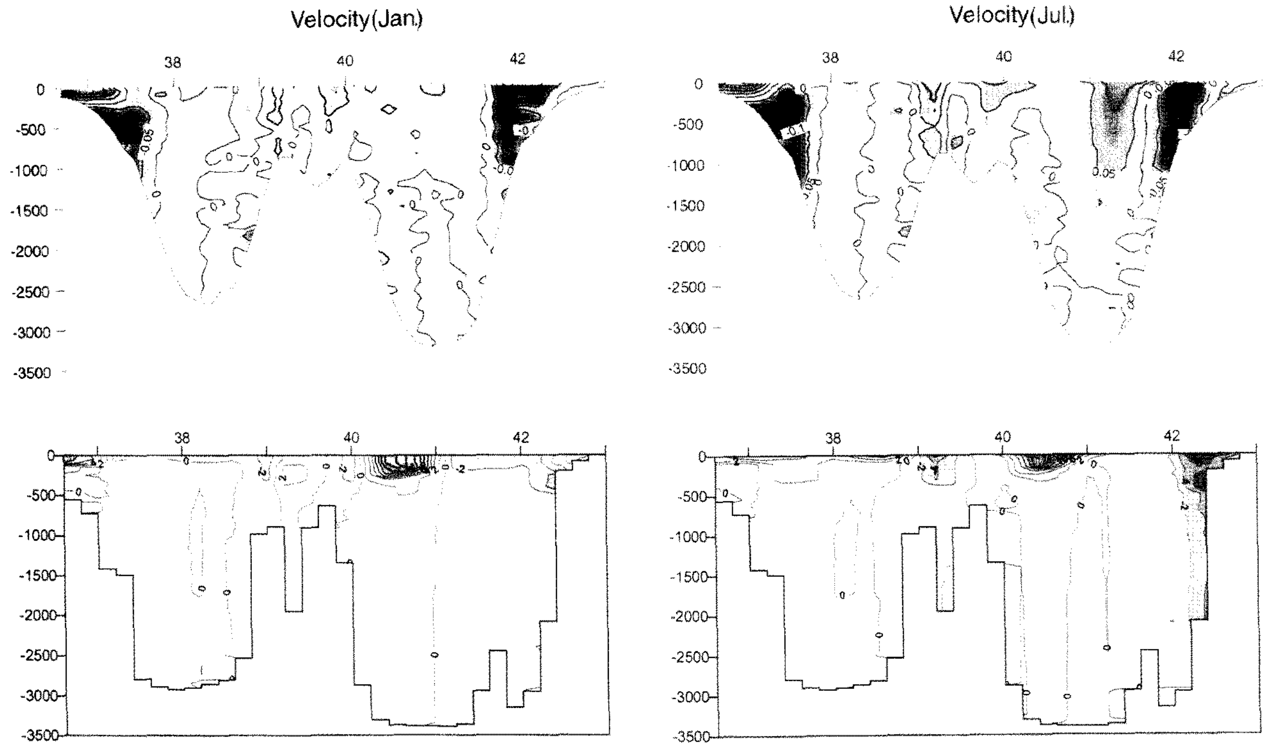

Fig. 6. Distribution of normal component of current velocity on the vertical section along PM line for POM (upper) and MICOM (lower) in January and July; units are m/sec for POM and cm/sec for MICOM. Ordinate is in meter and abscissa is in°N. Red and blue denote, respectively, northward and southward currents.

western boundary. The amount of low salinity water on this section is much smaller than that obtained by KS. This may be a consequence of the reduced southward intrusion of the low salinity water due to the different wind climatology used here. The velocity section (Fig. 8) indicates that this water moves slowly to the south. An accumulation of warm water near Ulleung Island, so called Ulleung Warm Lens (Kang and Kang 1990), is observed near 130°E. As reported by Shin *et al.* (1995), an anticyclonic recirculation with relatively deep structure exists around the Warm Lens (see Fig. 8). Similar anticyclonic eddy seems to develop in POM, but is not clearly defined. The high salinity TC water develops in summer near the surface in the eastern half of the section in POM, that reflects the development of NB, although it is not well defined in horizontal plane (Fig. 8). The TC water always develops in the western half of the section in MICOM, indicating that the NB does not develop strong enough in summer, as can be seen in the horizontal distribution of the surface current. Surface currents are vertically exaggerated at some locations in POM, especially near 133.5°E where the surface current with magnitude 5 cm/s reaches down to 1000 m depth. It is not understood why it occurs, and it should be removed or mitigated in future modeling.

4. Concluding remarks

Although this study is preliminary, many differences are found between POM and MICOM. Details of these differences cannot be explained at present mainly because we do not have sufficient observational data to compare with. Nevertheless, it can be said that MICOM has a great advantage over POM in that it reproduces well the isopycnic processes which are dominant in most of ocean interiors, especially the structure of intermediate/deep water masses and their movements related to thermohaline processes. This aspect of MICOM is quite important when considering that most of intermediate/deep circulations are closely related to density structure. In fact, the distribution and circulation of the low salinity water, the ESIW, obtained in MICOM

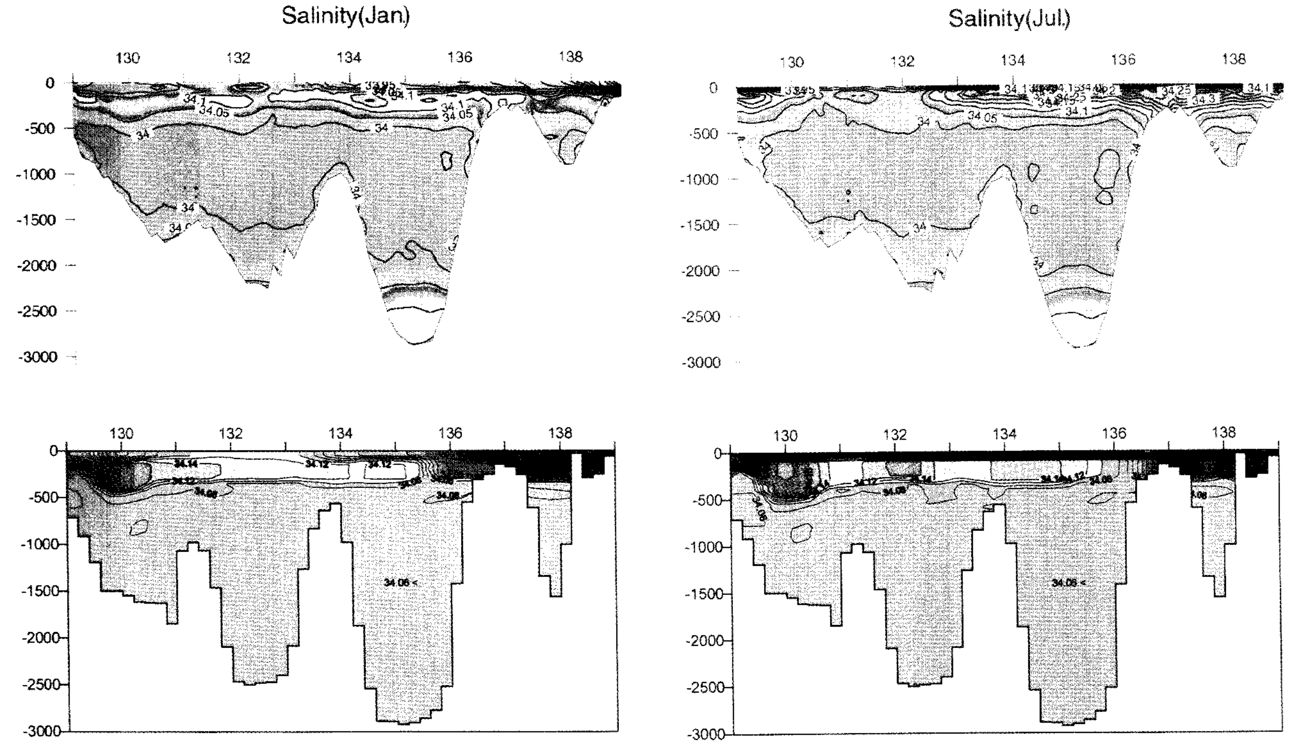

Fig. 7. Same as Fig. 5 except for 106 line. Abscissa is in°E.

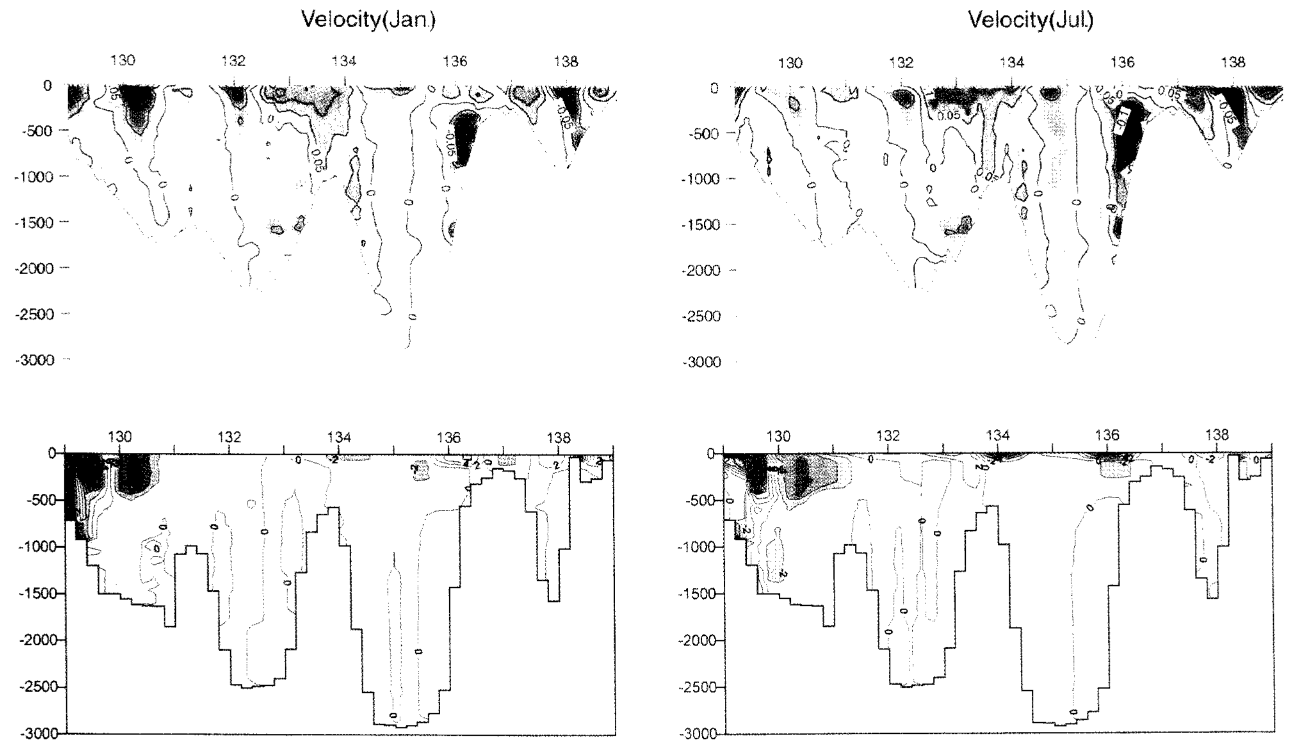

Fig. 8. Same as Fig. 6 except for 106 line. Abscissa is in°E.

seem to be quite successful except for the limitation of its southward penetration presumably due to the wind forcing applied here. On the other hand, present MICOM is not suitable in reproducing the surface currents accurately because it cannot have the fine vertical resolution in the upper layer. As a result, the NB and NKCC/CC obtained in MICOM are not so realistic. To reproduce these currents properly, MICOM should be modified so that it can have sufficient thin vertical layers which matches with the imposed open boundary conditions.

POM has no limit in the vertical resolution of the upper layer, hence allowing the accurate surface currents. The surface current patterns obtained by POM are generally more realistic than those obtained by MICOM, although there appear some unrealistic features such as the broad model EKWC, the seasonal changes of the EKWC and NKCC/LC not the same as those expected, and the unusually thick TC layer. The broad EKWC may be in part due to the larger horizontal eddy viscosity, and the unexpected seasonal changes of the EKWC and NKCC/LC are thought to partly come from the wind climatology employed here. However, it is not understood why the TC layer is unrealistically thick in POM. The failure in imposing the conditions suitable to the East Sea may also partly result in these unrealistic features because this model focuses on the entire Northwestern Pacific rather than the East Sea alone. Previous results obtained by using z-coordinate models (e.g. Seung and Kim 1993; Kim and Yoon 1999), which considers the East Sea only, do not show the unrealistic features mentioned above. Hence, a question arises whether this difference comes from the difference in numerical scheme or from the difference in imposed conditions. Those questions could be answered in future study by including, on the one hand, the z-coordinate model into the inter-comparison and, on the other hand, by taking the same model domain for all the models considered. Both POM and MICOM fail to produce strong deep currents as observed by Takematsu *et al.* (1999) probably because horizontal grid resolutions are not fine enough.

Acknowledgements

This study is funded partly by Korea Ocean Research and Development Institute (BSPM 0005-00-1291-1) and Inha University(2000). We would like to thank Prof. Y.J. Ro and Dr. C.H. Kim for their comments that greatly improved this paper.

References

Bryan, K. and M.D. Cox. 1969. A numerical investigation of the oceanic general circulation. *Tellus,* 14, 54-80.

Cox, M.D. 1984. A Primitive Equation, Three-dimensional Model of the Ocean. Tech. Rep. No. 1, Ocean Group, GFDL, Princeton, 143 p.

Chu, P., L. Jian, and H. Strauhs. 1999. A numerical simulation of the Japan/East Sea (JES) seasonal circulation. p. 94-105. In: *Proceedings of 6th International Conference Estuarine and Coastal Modeling,* New Orleans, USA, Nov. 3-5. American Society of Civil Engineering.

Hase, H., J.H. Yoon, and W. Koterayama. 1999. The current structure of the Tsushima Warm Current along the Japanese coast. *J. Oceanogr.,* 55, 217-235.

Hogan, P.J. and H.E. Hurlbert. 2000. Impact of upper ocean-topographical coupling and isopycnal outcropping in Japan/East Sea models with 1/8° to 1/6° resolution. *J. Phys. Oceanogr.,* 30, 2535-2561.

Holloway, G., T. Sou, and M. Eby. 1995. Dynamics of circulation of the Japan Sea. *J. Mar. Res.,* 53, 539-569.

Isobe, A. and Y. Isoda. 1997. Circulation in the Japan Basin, the northern part of the Japan Sea. *J. Oceanogr.,* 53, 373-381.

Kang, H.E. and Y.Q. Kang. 1990. Spatio-temporal characteristics of the Ullung Warm Lens. *Bull. Korean Fish. Soc.,* 23, 407-415.

Kawabe, M. 1982. Branching of the Tsushima Current in the Japan Sea. Part II : Numerical experiment. *J. Oceanogr. Soc. Japan,* 38, 183-192.

Kim, K. and J.Y. Chung. 1984. On the salinity minimum layer and dissolved oxygen-maximum layer in the East Sea (Japan Sea). p. 55-65. In: *Ocean Hydrodynamics of the Japan and East China Seas,* ed. by T. Ichiye. Elsevier, Amsterdam.

Kim, K.R. and K. Kim. 1996. What is happening in the East Sea (Japan Sea)?: Recent chemical observations during CREAMS 93-96. *J. Korean Soc. Oceanogr.,* 31, 164-172.

Kim, K., K.R. Kim, Y.G. Kim, Y.K. Cho, J.Y. Chung, B.H. Choi, S.K. Byun, G. H. Hong, M. Takematsu, J.-H. Yoon, Y. Volkov, and M. Danchenkov. 1996. New findings from CREAMS observations: Water masses and eddies in the East Sea. *J. Korean Soc. Oceanogr.,* 31, 155-163.

Kim, C.H., H.-J. Lie, and K.S. Chu. 1991. On the intermediate water in the southwestern East Sea (Sea of Japan). p.

129-141. In: *Oceanography of Asian Marginal Seas,* ed. by K. Takano. Elsevier, Amsterdam.

Kim, K.J. and Y.H. Seung. 1999. Formation and movement of the ESIW as modeled by MICOM. *J. Oceanogr.,* 55, 369-382.

Kim, C.H. and J.H. Yoon. 1999. A numerical modeling of the upper and intermediate layer circulation in the East Sea. *J. Oceanogr.,* 55, 327-345.

Kraus, E.B. and J.S. Turner. 1967. A one-dimensional model of the seasonal thermocline.Part II: The general theory and its consequences. *Tellus,* 19, 98-105.

Lee, D.K., J.C. Lee, S.R. Lee, and H.-J. Lie. 1997. A circulation study of the East Sea using satellite-tracked drifters. 1: Tsushima Current. *J. Korean Fish. Soc.,* 30, 1021-1032.

Lie, H.-J., M.S. Suk, and C.H. Kim. 1989. Observations of southeastward deep currents off the east coast of Korea. *J. Oceanol. Soc. Korea,* 24, 63-68.

Mellor, G.L. and A.F. Blumberg. 1985. Modelling vertical and horizontal diffusivities and the sigma coordinate system. *Mon. Wea. Rev.,* 113, 1379-1383.

Moriyasu, S. 1972. The Tsushima Current. p. 353-369. In: *Kuroshio - Its Physical Aspects,* eds. by H. Stommel and K. Yoshida. Univ. Tokyo Press, Tokyo.

Ro, Y.J. 1999. Numerical modeling experiment of the East (Japan) Sea circulation and mesoscale eddy generation based on POM-ES. p. 1167-1181. In: *Proceedings of 6th International Conference Estuarine and Coastal Modeling,* New Orleans, USA, Nov. 3-5. American Society of Civil Engineering.

Senjyu, T. 1999. The Japan Sea Intermediate Water; Its characteristics and circulation. *J. Oceanogr.,* 55, 111-122.

Senjyu, T. and H. Sudo. 1993. Water characteristics and circulation of the upper portion of the Japan Sea Proper Water. *J. Mar. Sys.,* 4, 349-362.

Senjyu, T. and H. Sudo. 1994. The Upper Portion of the Japan Sea Proper Water; Its source and circulation as deduced from isopycnal analysis. *J. Oceanogr.,* 50, 663-690.

Seung, Y.H. 1992. A simple model for separation of East Korean Warm Current and formation of North Korean Cold Current. *J. Oceanol. Soc. Korea,* 27, 189-196.

Seung, Y.H. and K. Kim. 1993. A numerical modeling of the East Sea circulation. *J. Oceanol. Soc. Korea,* 28, 292-304.

Seung, Y.H. and J.H. Yoon. 1995a. Some features of winter convection in the Japan Sea. *J. Oceanogr.,* 51, 61-73.

Seung, Y.H. and J.H. Yoon. 1995b. Robust diagnostic modeling of the Japan Sea circulation. *J. Oceanogr.,* 51, 421-440.

Shin, H.R., S.K. Byun, C.S. Kim, S.C. Hwang, and C.W. Shin. 1995. The characteristics of structure of warm eddy observed to the northwest of Ullungdo in 1992. *J. Korean Soc. Oceanogr.,* 30, 39-56.

Takematsu, M., Z. Nagano, A.G. Ostrovskii, K. Kim, and Y. Volkov. 1999. Direct measurements of deep currents in the northern Japan Sea. *J. Oceanogr.,* 55, 207-216.

Yoon, J.H. 1982a. Numerical experiment on the circulation in the Japan Sea. Part I. Formation of the East Korean Warm Current. *J. Oceanogr. Soc. Japan,* 38, 43-51.

Yoon, J.H. 1982b. Numerical experiment on the circulation in the Japan Sea. Part II. Influence of seasonal variations in atmospheric conditions on the Tsushima Current. *J. Oceanogr. Soc. Japan,* 38, 81-94.

Yoon, J.H. 1982c. Numerical experiment on the circulation in the Japan Sea. Part III. Mechanism of the Nearshore Branch of the Tsushima Current. *J. Oceanogr. Soc. Japan,* 38, 125-130.

Yoshikawa, Y., T. Awaji, and K. Akitomo. 1999. Formation and circulation processes of Intermediate Water in the Japan Sea. *J. Phys. Oceanogr.,* 29, 1701-1722.

Received May 4, 2001
Accepted Jun. 30, 2001